One-on-one pure pursuit with intermittent locomotion

Research project

Author: Dekel Fishler
Advisor: Prof. Tal Shima

The Cooperative Autonomous Systems (CASY) Lab
Faculty of Aerospace Engineering, Technion

November 2024

Abstract

In order for the pursuer to hit the target, it must be capable of controlling its movements. Flying animals are similar to guided missiles in the way that they adjust their movements constantly. However, animals that are not capable of flying toward their targets, such as marine animals, may pause their movements during the pursuit of their prey. This project was based upon the pursuit strategy of Zebrafish, and explored how intermittent pure pursuit movement affects the pursuit process and its outcome. The guidance concept is based on the geometric principle of pure pursuit, with acceleration stops planned perpendicular to the pursuer's velocity vector during the pursuit process. Different pursuer speeds and various target positions were introduced to demonstrate the implementation. In addition, we developed a method for preventing overshoot at the end of the scenario, as well as a ratio that ensures target capture.

Contents

1 Nomenclature

γ_M	Interceptor path angle
γ_T	Target path angle
δ	Interceptor look angle, the angle between LOS to the interceptor velocity
λ	LOS angle
λ_P^i, λ_Z^i	λ at the i-th stage of PP and IPP, respectively
μ	The ratio between t_p and t_z at which the pursuer will hit the target
θ	Target look angle, the angle between LOS to the target velocity
θ_P^i, θ_Z^i	θ at the i-th stage of PP and IPP, respectively
a_M	Lateral acceleration of interceptor
a_T	Lateral acceleration of target
i	The number of times the PP and IPP coupling was performed
K	The ratio of the interceptor's speed to the target's speed
M	Interceptor mark
r	Range between the target and the interceptor
r_P^i, r_Z^i	Range at the i-th stage of PP and IPP, respectively
(r_{xZ}^i, r_{yZ}^i)	x and y coordinates of the range, respectively at the i-th stage of IPP
t	Time from launch
t_i	Time from the beginning of the i-th stage
t_p	The duration of pure pursuit
t_z	The duration of the delay in pure pursuit
T	Target mark
V_M	Interceptor speed
V_T	Target speed
(X_M, Y_M)	x and y coordinates of the interceptor, respectively
(X_T, Y_T)	x and y coordinates of the target, respectively
IPP	Intermittent Pure pursuit
IPP_s	Intermittent Pure pursuit stage
LOS	Line of sight
PP	Pure pursuit
PP_s	Pure pursuit stage
X–O–Y	Inertial Cartesian reference frame

2 Introduction

In missile guidance, the interceptor's trajectory is planned towards a predetermined target, whether it is stationary or moving. In general, the guidance problem consists of two levels, geometric rule and guidance rule. The geometric law describes the desired kinematics between the pursuer and the target. Pure pursuit (PP) is a simple example of a geometric law. This law is based on the idea that the velocity vector of the pursuer ($\mathbf{v_M}$) coincides with the vector between the pursuer and the pursued $\mathbf{r}$. Parallel navigation is another geometric rule, in which the pursuer must keep the direction of the 'line-of-sight' (LOS) constant relative to the inertial space. These two rules are part of a set of rules that requires two points, the pursuer and the target. There are also geometric rules that require three points, meaning that in addition to the pursuer and the target, there is another reference point. An example of this type of geometrical rule is called LOS guidance which requires the pursuer to be constantly on LOS between the target and a reference point.

The second level is a guidance law, which is the implementation of the geometrical rule, An example of guidance law is proportional navigation (PN), where with lateral acceleration that is proportional to the rate of change of the LOS it is possible to implement the parallel navigation geometrical rule. [1]

The development of both defense and attack technologies has accelerated in recent decades, requiring advanced guidance laws beyond the traditional PN law. Nowadays, additional requirements exist such as impact angle control and multi-missile attacks. An important parameter in the pursuit problem is the impact time, and one of the earliest papers on the topic is [2], which proposes a closed-form solution based on the PN and feedback on the impact time error, which is defined as the difference between the approximated impact time from PN and the desired impact time. A more accurate estimate of impact time was achieved by utilizing higher-order terms in subsequent research [3] using the nonlinear formulation.

As part of the discussion of time of impact, the term "time-to-go" (t_{go}) represents the remaining time until the collision occurs. It is possible to estimate this time in several different ways, including range-over-range rates, but this method is only accurate if there is a small amount of direction error relative to the collision path. A method for estimating t_{go} has been proposed in [4] by updating the time estimate noniteratively. Using this method, a simple and clear estimate of t_{go} is obtained for PN and augmented PN applications.

An algorithm for estimating the time to target based on the guidance command history was presented in the [5] research, where an algorithm was proposed to estimate the time until impact. It is possible to develop a Taylor series expansion for the expression t_{go} containing a trigonometric function. [6] presents a method for determining the impact time for PN to a static target using interpolation. [4]-[6] are methods to estimated the t_{go} but did not control the impact time.

Regarding the methods for influencing impact time, the suggested guidance laws based on sliding mode control were proposed in [7] in order to impact the target at a desired time. Several types of targets were evaluated, including stationary and constant velocity targets. According to the study [8], impact time is defined as a beta function influenced by initial conditions and controlled by a single parameter. By applying a polynomial shape to the look-angle profile for a static target in [9], they were able to control impact time. Further research [10] extended the polynomial method to cover changes in target velocity as well.

Furthermore, there are studies that propose methods for controlling the impact angle in conjunction with the impact time, in addition to enforcing a specific impact time. As an example of such a scenario, [11] introduces a guidance concept based on geometric principles that constrain the interceptor to follow a circular trajectory toward the target as a result of the geometric principle. By scheduling the interceptor's launch, the desired impact time and angle can be enforced. There is also a guidance law proposed in [12] that is aimed at leading a vehicle to a target at a predetermined impact time with a predetermined impact angle at a desired impact time. A feedback loop is included in the law to achieve the desired impact angle, as well as an additional control command to control the impact time. As proposed in [13], a guidance law based on a polynomial of the guidance command with three unknown coefficients is proposed. There is a coefficient that is determined to achieve the desired impact time, and the remaining coefficients are determined to meet the constraint of the final impact angle and to ensure zero miss distance.

2.1 Nature Inspired Methods

In science and engineering, biological systems have long served as sources of inspiration. Among the reasons for studying animal behavior in nature are to gain an understanding of the natural world and to find solutions to complex problems in a variety of fields not necessarily related to natural behavior. The study of animals has developed an area of study that focuses on hunting behavior and attempts to describe this behavior according to currently known guidance laws.
An analysis of the attack process of a hawk on an erratically maneuvering prey is presented in the article [14]. During the attack, the researchers divided the hawk's movements into two components: a PP with a short delay in time, and a PN guidance law.
According to the article [15], the peregrine falcon differs from the hawk in that it uses a PN guidance law that has a low gain N (feedback gain that is called the navigation constant) when compared to the hawk. Based on many experiments, it has been determined that median $N = 2.6$; first, third quartiles: 1.5, 3.2 for attacking stationary and maneuvering targets. This coefficient is adapted to the peregrine falcon's relatively low flight speed. A follow-up study [16] has found that naive gyrfalcons also use the PN guidance law, but operate at significantly lower N values than peregrine falcons. The median $N = 1.2$; the first and third quartiles were 0.5, 1.4 . The difference results in slower turns and a longer path to the target.
In [17], an interesting phenomenon in insects that seek to camouflage their motion while approaching or escaping from another insect was investigated. The concept of motion camouflage is that the pursued insect perceives the pursuing insect as if it were stationary at a fixed point, while in reality, it is approaching. This study demonstrated a connection between this motion camouflage behavior and PN. According to the research [18], bats also use this method of PN, which causes the pursuer to "appear" stationery.
It has already been mentioned that some animals use PP, like the hawk. The method has also been observed in tiger beetles [19], as well as houseflies [20]. Animals use a variety of guidance laws as well, and they differ slightly from PP. During chasing, bluefish [21] use deviated PP methods. For the fish to successfully utilize this strategy of PP or a method based on PP, it requires a minimal amount of information and a relatively low level of motor coordination, which appears to suit the fish's aquatic environment. Another species that uses PP is the Zebrafish [22], which performs bursts of rapid movement interspersed with pauses. According to the research, the guidance law for the Zebrafish was identified as intermittent PP (IPP), which is based on the intermittent movements of the predator.
In this project, we drew inspiration from the pursuit strategy of Zebrafish. We found this method to be intriguing because it is unclear how the intermittent movement benefits the fish, in terms of the t_{go} or in terms of the energy the fish must exert with this method compared to PP.
The project is structured as follows: First, a review of the relevant topics is presented, followed by the fundamental definitions and the formulation of the guidance problem in Cartesian coordinates. Next, numerical simulations concerning a scenario of a moving but non-maneuvering target are shown. Finally, conclusions are drawn.

3 Problem Formulation

A planar interception problem is treated. Presenting basic definitions from the field of guidance as a background for formulating the guidance problem relevant to the IPP applicable to this article.

3.1 Engagement Description

The schematics in Fig. 1 present the planar engagement geometry. The X–O–Y axes form the flat-Earth inertial Cartesian reference frame M and T denote the positions of interceptor, and target, respectively.
The line-of-sight angles between the pairs interceptor–target, denoted by LOS. The distances between the pairs are denoted by r. V_M and V_T are the speeds of the interceptor and the target, respectively, assumed to be constant. γ_M and γ_T are the path angles of the interceptor and the target, respectively. δ is the interceptor lead angle and θ is the target lead angle. The line-of-sight angles between LOS and the reference axis X are denoted as λ.

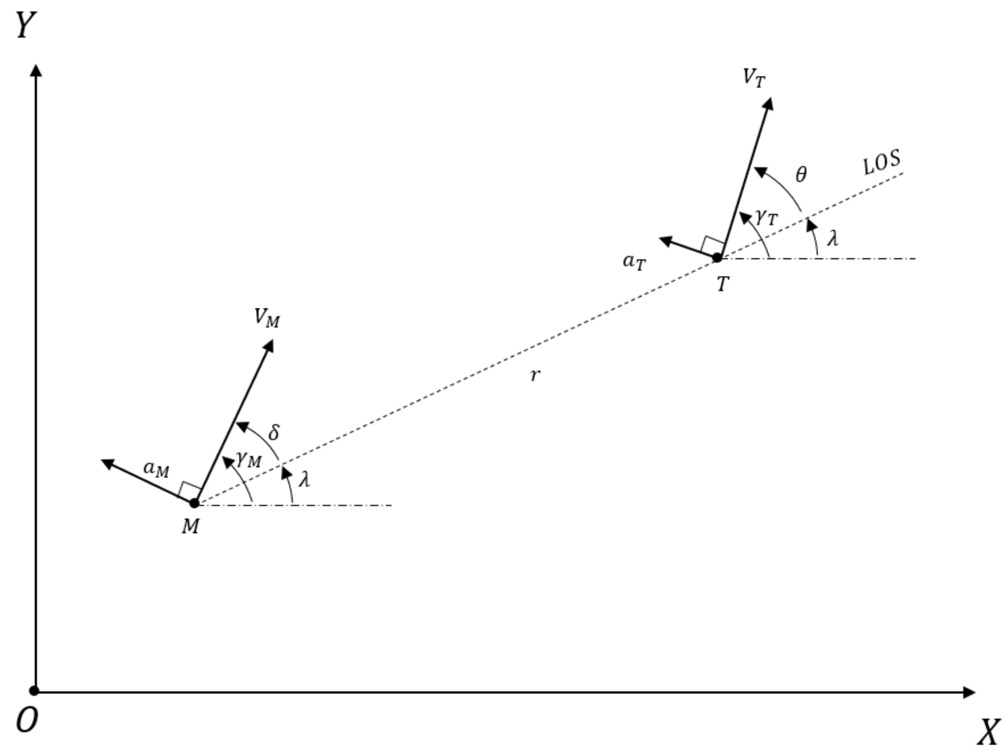

Figure 1: Schematic of planar engagement

Neglecting the gravitational force, the nonlinear engagement kinematics equations of the interceptor, expressed in the inertial Cartesian coordinate system, are as follows:

$$\begin{cases} \dot{X}_M &= V_M \cos(\gamma_M(t)) \\ \dot{Y}_M &= V_M \sin(\gamma_M(t)) \\ \dot{\gamma}_M(t) &= \frac{a_M(t)}{V_M} \end{cases} \tag{1}$$

The kinematics equations of the target:

$$\begin{cases} \dot{X}_T &= V_T \cos(\gamma_T(t)) \\ \dot{Y}_T &= V_T \sin(\gamma_T(t)) \\ \dot{\gamma}_T(t) &= \frac{a_T(t)}{V_M} \end{cases} \tag{2}$$

3.2 Guidance Concept

In this subsection, the geometric concept is outlined. The goal is to reach the target by applying IPP, meaning that PP is applied for a set period, this stage will be referred to as PP_s. After which the interceptor continues to move in a straight line for another set period, this stage will be referred to as IPP_s. and the process repeats itself. Let i denote the number of times the coupling PP and IPP was performed, t_i represents the time from the beginning of the $i-th$ stage and t_p, t_z will be the duration of PP_s and IPP_s, respectively.
In order for the pursuer to catch the target, the pursuit must end with a phase of PP. The acceleration will be of the following form:

$$a_M = \begin{cases} a_{M_p} & (t_p + t_z)(i-1) < t_i \leq (i-1)t_z + i \cdot t_p \\ 0 & (i-1)t_z + i \cdot t_p < t_i \leq (t_p + t_z) \cdot i \end{cases} \tag{3}$$

The objective of PP is to ensure that the interceptor's velocity vector V_M points directly at the target's location, meaning that δ is equal to 0. The clear advantage of PP is that it requires minimal information (only the target's location needs to be known).
The angle δ, as shown in Fig. 1, is the angle between the V_M and LOS. We will assume that this angle is zero for PP, and additionally, we will assume that the target is not maneuvering ($a_T = 0$). Throughout the article, there is an ideal dynamic model of the interceptor.

3.2.1 Kinematics of PP_s

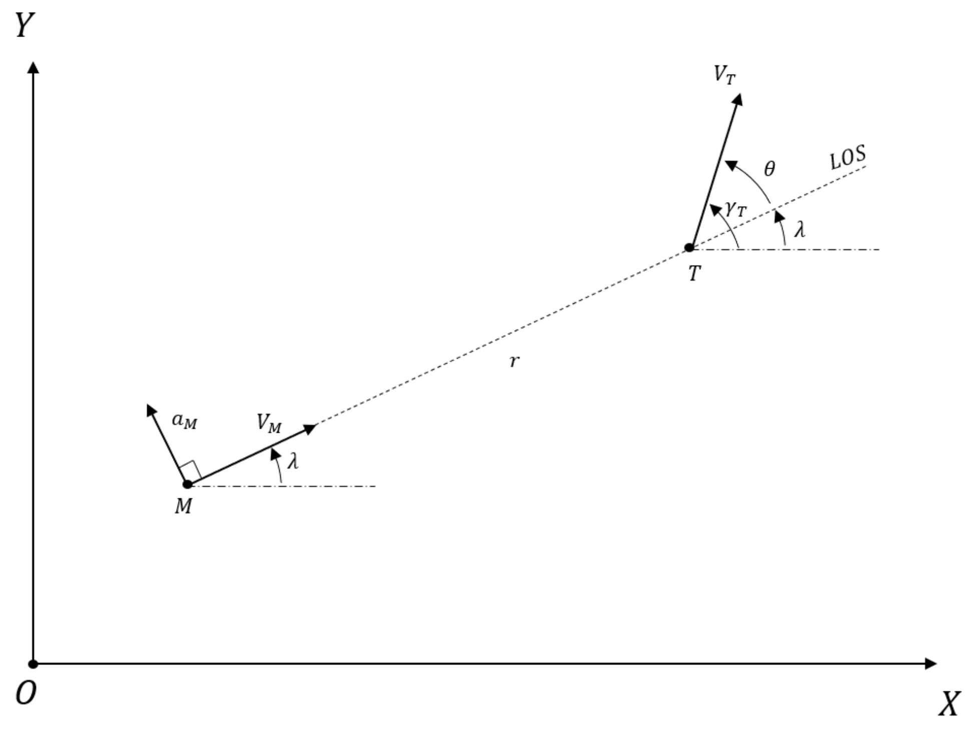

Figure 2: Schematic of planar PP

Since $a_T = 0 \quad \Rightarrow \quad \dot{\gamma}_T = 0$ by assumption (as T is not maneuvering) it follows that:

$$\dot{\gamma}_T = \dot{\theta} + \dot{\lambda} \quad \underset{\dot{\gamma}_T = 0}{\Rightarrow} \quad \dot{\theta} = -\dot{\lambda} \tag{4}$$

The equations of motion for the PP_s that are shown in Fig. 2 will be:

$$\begin{cases} \dot{r} = V_T \cos\theta - V_M \\ \dot{\theta} = -\dot{\lambda} = -\frac{V_T}{r} \sin\theta \end{cases} \tag{5}$$

K is defined as

$$K = \frac{V_M}{V_T} \tag{6}$$

Assuming that K is constant

$$\frac{dr}{d\theta} = \frac{r(K - \cos\theta)}{\sin\theta} \tag{7}$$

By separation of variables and integration, the solution to Eq.(7) is found to be

$$r(\theta) = D \cdot \frac{sin^{K-1}\frac{\theta}{2}}{2cos^{K+1}\frac{\theta}{2}} = D \cdot \frac{tan^{K}\frac{\theta}{2}}{sin\theta} \tag{8}$$

Where D is a constant.

From time integration of Eq.(5)

$$t = \frac{r_0}{V_T} \cdot \frac{K + cos\theta_0 - (\frac{r}{r_0}) \cdot (K + cos\theta)}{K^2 - 1} \tag{9}$$

At the end of IPP_s, the angle $\delta \neq 0$. For PP, it is necessary to bring δ to zero. For this, the pursuer will apply an acceleration that will be $\vec{a}_M \perp \vec{V}_M$, and its magnitude will be:

$$a_{M_p} = -CV_M^2 sin\delta \tag{10}$$

Where C is a constant.

3.2.2 Kinematics of IPP_s

When the PP_s ends, the pursuer transitions to the IPP_s phase, where at the beginning, $\delta = 0$ will be 0, and as t_i increases, the absolute value of δ will also increase. In Fig. 3, the planar engagement geometry between the pursuer and the target is shown.

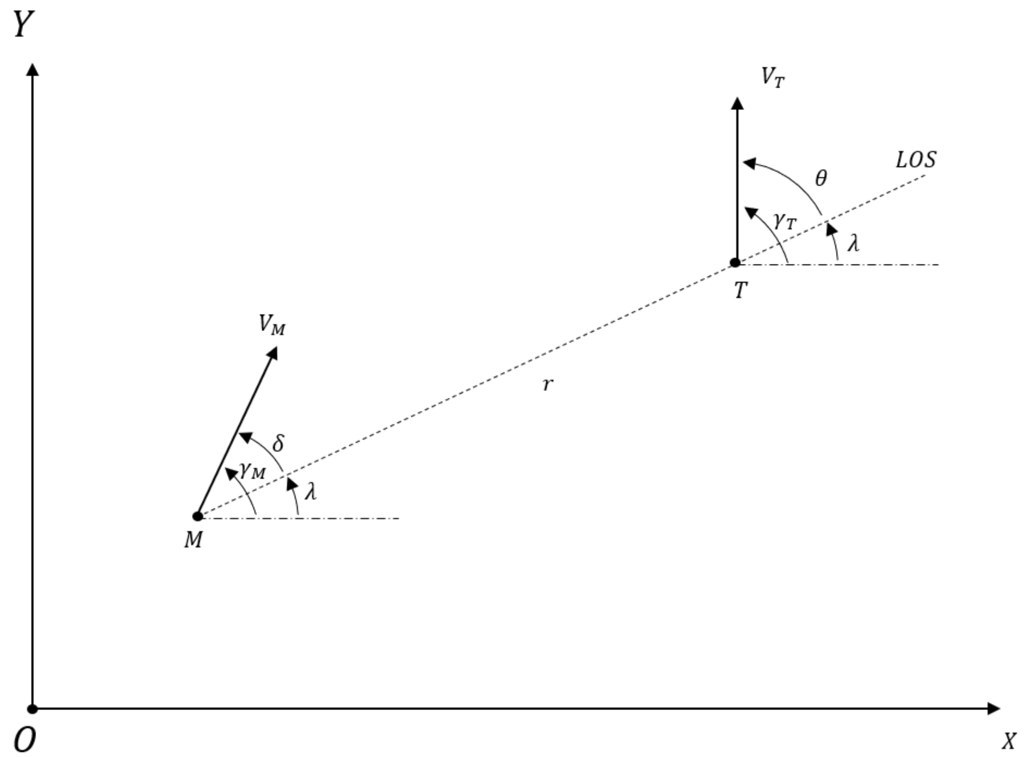

Figure 3: Schematic of planar IPP_s

It can be noted that $a_T = 0$ and $a_M = 0, \quad \Rightarrow \quad \dot{\gamma}_M = 0, \quad \dot{\gamma}_T = 0.$

$$\begin{cases} \gamma_M = \lambda + \delta = const \\ \gamma_T = \lambda + \theta = const \end{cases} \tag{11}$$

The equations of motion for the IPP_s will be:

$$\begin{cases} \dot{r} = V_T \cos\theta - V_M \cos\delta \\ \dot{\theta} = -\dot{\lambda} = \frac{1}{r}(-V_T \cdot sin\theta + V_M \cdot sin\delta) \end{cases} \tag{12}$$

Hence the differential equation

$$\frac{dr}{d\theta} = \frac{r(\cos\theta - K\cos\delta)}{-\sin\theta + K\cos\delta} \tag{13}$$

4 Simulations of IPP and PP

It can be expected that, as with PP, also in the case of IPP, the larger the ratio K, the faster the interceptor will reach the target.
The scenario includes one interceptor against a non-maneuvering target. The interceptor is launched from $(X_{M_0}, Y_{M_0}) = (0, 0)$ with varying speed $V_M \left[\frac{M}{S}\right]$ and path angles which are equal to $\gamma_M(0) = 90\,[deg]$. The target is launched from $(X_{M_0}, Y_{M_0}) = (0, 6000[m])$ with speed of $V_T = 100\left[\frac{M}{S}\right]$ and path angles which are equal to $\gamma_T(0) = 0\,[deg]$. The acceleration a_M is unbounded. Fig. 4 presents the simulation.

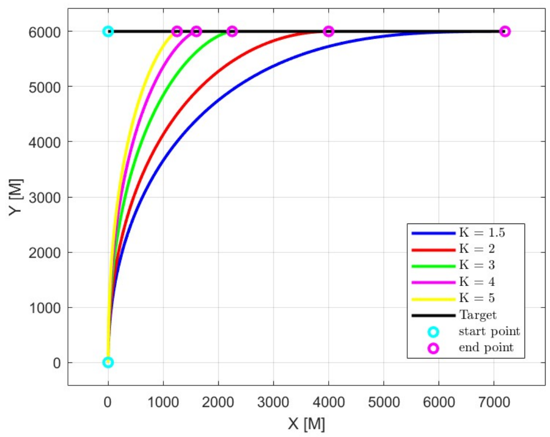

(a) Trajectories for different K, PP

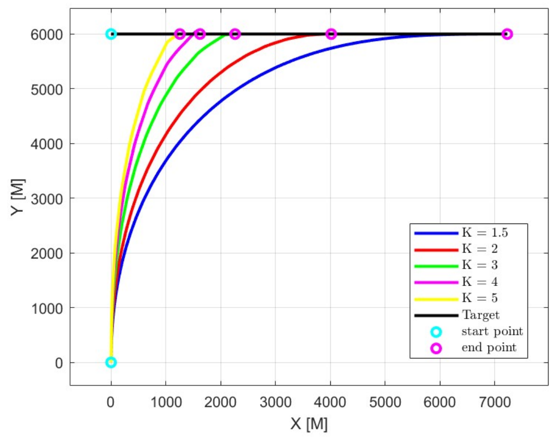

(b) Trajectories for different K, $t_p = 1$, $t_z = 1$

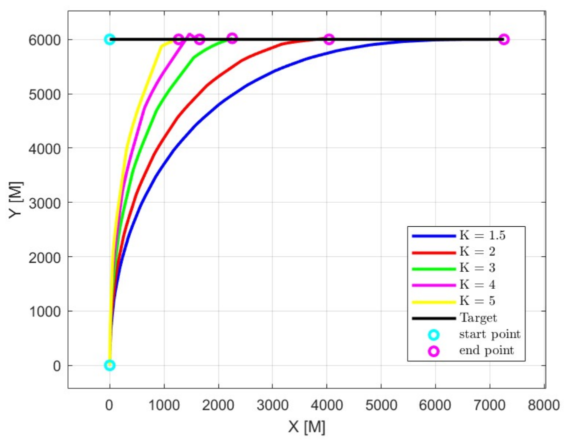

(c) Trajectories for different K, $t_p = 2$, $t_z = 2$

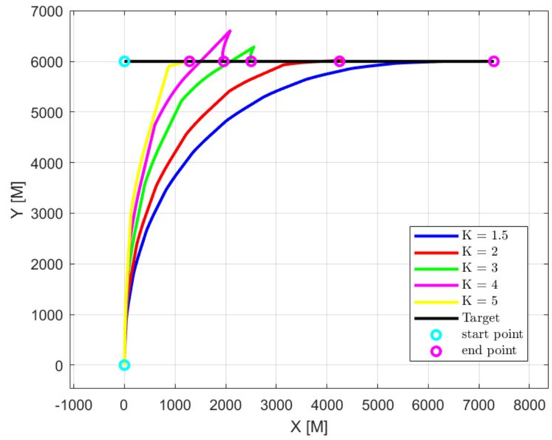

(d) Trajectories for different K, $t_p = 3$, $t_z = 3$

Figure 4: Trajectories for different K and t_p, t_z

4.1 Discussion

It can be noted that as K increases, the pursuer indeed hits the target earlier. Additionally, when using the IPP method, the pursuer will catch the target later than with the PP method. It can also be observed that the probability of the pursuer making a significant overshoot, that is, passing the target and then catching up to it, increases as K increases. However, this is not always the case, as shown in Figures 4b-4d for K = 5. Furthermore, we will notice that as t_p, t_z increases although the ratio $\frac{t_p}{t_z}$ remains constant, it is possible that the pursuer will make a larger overshoot.

5 Guaranteeing target capture

A lower bound is found for which the pursuer will hit the target with certainty.
From Eq.(12):

$$\dot{r} = V_T \cos\theta - V_M \cos\delta$$

In order to find a lower bound:

$$\dot{r} = V_T \cos\theta - V_M \cos\delta \quad \underset{\delta=180^\circ}{\Rightarrow} \quad \dot{r} = V_T \cos\theta + V_M$$

The change in distance between the target and the pursuer in this case will be:

$$\Delta r_z = \dot{r} \cdot t_z \quad \underset{\delta=180^\circ}{\Rightarrow} \quad \Delta r_z = (V_T \cos\theta + V_M) \cdot t_z$$

From Eq.(5):

$$\dot{r} = V_T \cos\theta - V_M \quad \Rightarrow \quad \Delta r_p = \dot{r} \cdot t_p$$

Since Δr_z is defined as positive, we will also require that Δr_p be positive.

$$\Delta r_p = -(V_T \cos\theta - V_M) \cdot t_p$$

To ensure reaching the target, we will require:

$$\Delta r_z \quad < \quad \Delta r_p \quad \Rightarrow \quad (V_T \cos\theta + V_M) \cdot t_z \quad < \quad (V_M - V_T \cos\theta) \cdot t_p$$

$$(\cos\theta + K) \cdot t_z \quad < \quad (K - \cos\theta) \cdot t_p$$

$$\frac{\cos\theta + K}{K - \cos\theta} \quad < \quad \frac{t_p}{t_z} \tag{14}$$

The variable μ is defined as:

$$\mu = \frac{\cos\theta + K}{K - \cos\theta} \tag{15}$$

For a $\frac{t_p}{t_z} > \mu$, the pursuit will intercept the target. For $K \leq 1$, the interceptor will not be able to reach the target, unless it is the singular case of head-on, in which adversaries fly toward each other. As shown in Fig. 5, the conditions for interception are determined by the angle θ for different values of K.

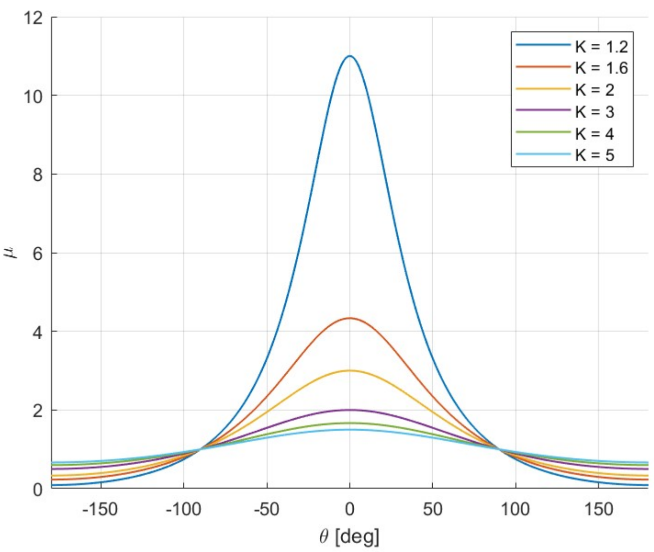

Figure 5: μ as a function of θ for different K values

5.1 Simulation

The engagement simulated in the section includes one interceptor against a non-maneuvering target. The interceptor is launched from $(X_{M_0}, Y_{M_0}) = (0, 0)$ with speed of $V_M = 200 \left[\frac{M}{S}\right]$ and path angles which are equal to $\gamma_M(0) = 0°$. The target is located at $(X_{M_0}, Y_{M_0}) = (5000[m], 0)$ with speed of $V_T = 100 \left[\frac{M}{S}\right]$ and path angles which are equal to $\gamma_T(0) = 90°$.
The acceleration a_M is unbounded. The simulation is presented in Fig. 6. The scenario is for different values of $\frac{t_p}{t_z}$.

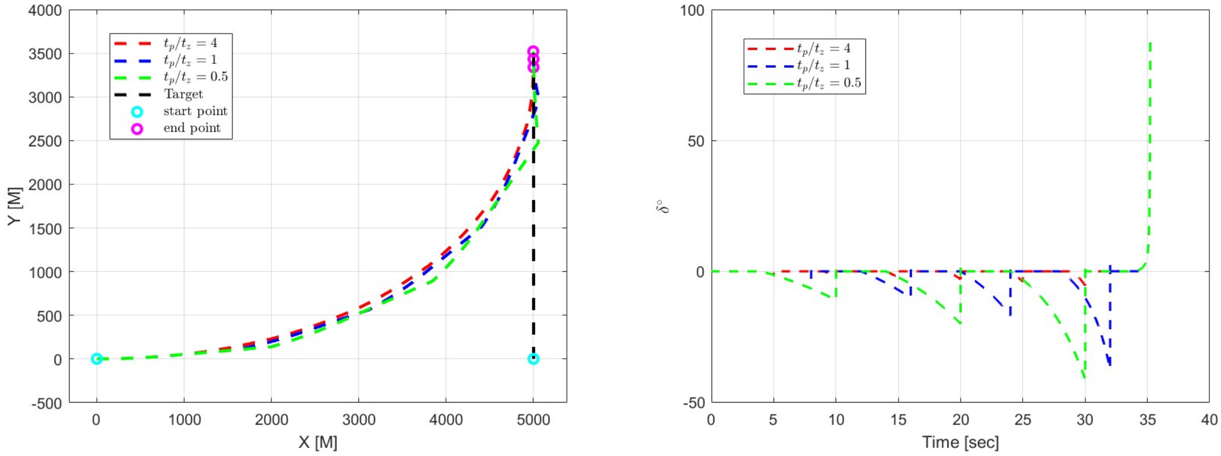

(a) Trajectories

(b) $\delta°$ As a function of time

Figure 6: Implementation of IPP for different ratio $\frac{t_p}{t_z}$.

5.2 Discussion

We defined interception of the target only when the scenario ends in PP. In the case presented in Fig.6 K =2. Thus, $\frac{t_p}{t_z} \geq \mu = 3$ ensures that the target is intercepted. It can be seen that for $\frac{t_p}{t_z} = 4$, the scenario ends in PP ($\delta = 0$ at the end of the scenario). It can be observed that even for $\frac{t_p}{t_z} = 1$, the scenario ends with PP. This result is appropriate because the ratio μ presented in Fig. 5 is not a tight bound, in the worst-case scenario, this ratio will ensure target interception, but interception is also possible at $\frac{t_p}{t_z} < \mu$. In contrast, for $\frac{t_p}{t_z} = 0.5$, it can be seen that the scenario does not end in PP ($\delta = 88.6°$ at the end of the scenario). This means that the pursuer will pass by the target. Indeed, the miss distance in this case will be 3.08 [m].

6 Boundary case analysis, $t_z \to 0$

In this chapter, we will examine the effect of reducing the time t_z on the IPP law.

6.1 Simulation

The engagement simulated in the section includes one interceptor against a non-maneuvering target. The interceptor is launched from $(X_{M_0}, Y_{M_0}) = (0, 0)$ with speed of $V_M = 100 \left[\frac{M}{S}\right]$ and path angles which are equal to $\gamma_M(0) = 0[deg]$. The target is located at $(X_{M_0}, Y_{M_0}) = (1000[m], 0)$ with speed of $V_T = 50 \left[\frac{M}{S}\right]$ and path angles which are equal to $\gamma_T(0) = 90[deg]$. The acceleration a_M is unbounded. The simulation is presented in Fig. 7.

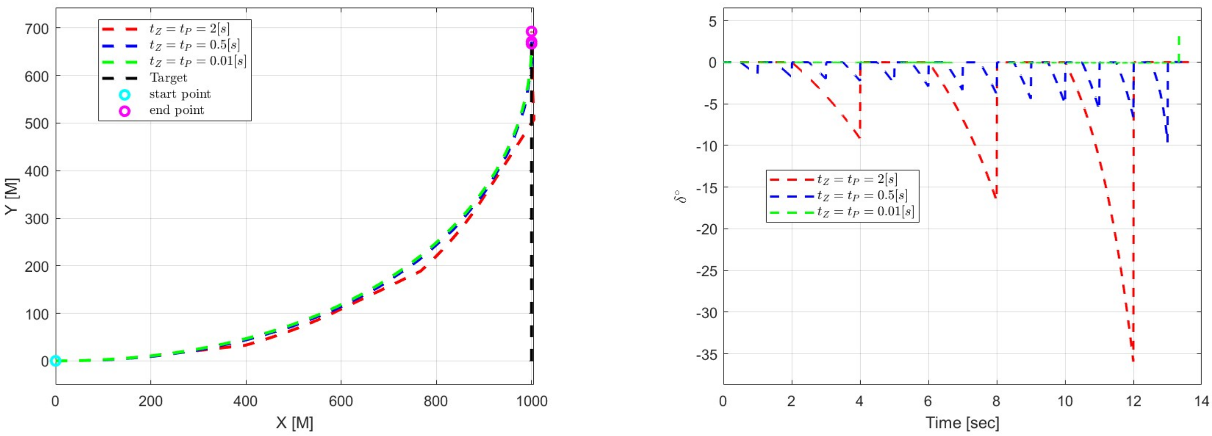

(a) Trajectories (b) δ° As a function of time

Figure 7: Implementation of IPP for different t_Z, t_P.

6.2 Discussion

During IPP_s:

$$\dot{\gamma}_M = \dot{\delta} + \dot{\lambda} \underset{\dot{\gamma}_M = 0}{\Rightarrow} \dot{\delta} = -\dot{\lambda}$$

$$\dot{\delta} = -\dot{\lambda} = \frac{1}{r}(-V_T \cdot sin\theta + V_M \cdot sin\delta) \tag{16}$$

Assuming that the scenario begins in a nominal PP_s where $\delta = 0$. As $t_Z \to 0$, we find that δ will not have time to change and will be $\delta \to 0$.
In this state, it can be seen that Eq.(12), which describes the motion during the IPP phase, will tend to become:

$$\begin{cases} \dot{r} = V_T \cos\theta - V_M \cos\delta & \rightarrow \quad \dot{r} = V_T \cos\theta - V_M \\ \dot{\theta} = -\dot{\lambda} = \frac{1}{r}(-V_T \cdot sin\theta + V_M \cdot sin\delta) & \rightarrow \quad \dot{\theta} = \frac{1}{r}(-V_T \cdot sin\theta) \end{cases} \tag{17}$$

Eq.(17) is essentially the equation of motion for PP_s, as described in Eq.(5). From this, we can conclude that, as shown in Fig. 7, for $t_Z \to 0$ the equations of motion will approach to PP $(\delta \to 0)$.

7 Overshoot Prevention

We would want to prevent overshooting by the interceptor for many reasons, such as a fuel shortage. In the case of PP, no overshoot will occur, but for IPP, there is a possibility that the interceptor will overshoot the target if, upon approaching the target, it is in a phase where IPP_s is happening. Fig. 4b-4d illustrates the overshoot in the pursuit process. To prevent this phenomenon, we would want the pursuer to reach the target with PP_s so that the interceptor can capture the target. If the interceptor is in the IPP_s when it reaches the target, it will overshoot and pass the target.
Definitions:

$$\begin{cases} \lambda_P^i, \lambda_Z^i & \lambda \text{ at the i-th stage of PP and IPP, respectively} \\ \theta_P^i, \theta_Z^i & \theta \text{ at the i-th stage of PP and IPP, respectively} \\ r_P^i, r_Z^i & \text{Range at the i-th stage of PP and IPP, respectively} \\ (r_{x_Z}^i, r_{y_Z}^i) & \text{x and y coordinates of the range, respectively at the i-th stage of IPP} \end{cases} \tag{18}$$

The scenario begins with PP_s. based on Eq.(8) and Eq.(9)

$$\begin{cases} r_P^i(\theta) = D \cdot \dfrac{sin^{K-1}\left(\frac{\theta_P^i}{2}\right)}{2cos^{K+1}\left(\frac{\theta_P^i}{2}\right)} = D \cdot \dfrac{tan^K\left(\frac{\theta_P^i}{2}\right)}{sin(\theta_P^i)} \\ r_P^i(\theta) = \frac{r_{P_0}^i}{K+cos(\theta_P^i)} \cdot \left[K + cos(\theta_{P_0}^i) - \frac{V_T \cdot t_p(K^2-1)}{r_{P_0}^i} \right] \end{cases} \tag{19}$$

From the initial conditions of the i-th stage of PP_s, the constant D can be determined.
We have obtained two equations with two unknowns: the distance r and the angle θ.
For the first stage, the initial conditions are the interceptor's departure conditions, while for the subsequent stages, the initial conditions are the endpoint conditions of the IPP_s phase.

For the IPP_s phase :

$$\gamma_M = \lambda + \delta = const$$

The change in distance r will be:

$$\begin{cases} r_{x_Z}^i = r_{Z_0}^i \cdot cos(\lambda_{Z_0}^i) - V_M \cdot t_z \cdot cos(\lambda_{Z_0}^i) + V_T \cdot t_z \cdot cos(\gamma_T) \\ r_{y_Z}^i = r_{Z_0}^i \cdot sin(\lambda_{Z_0}^i) - V_M \cdot t_z \cdot sin(\lambda_{Z_0}^i) + V_T \cdot t_z \cdot sin(\gamma_T) \end{cases} \tag{20}$$

Where $r_{Z_0}^i$ and $\lambda_{Z_0}^i$ is the distance r and the angle λ at the end of the PP_s i-th stage respectively.

$$\begin{cases} r_Z^i = \sqrt{(r_{x_Z}^i)^2 + (r_{y_Z}^i)^2} \\ \lambda_Z^i = \arctan \frac{r_{y_Z}^i}{r_{x_Z}^i} \end{cases} \tag{21}$$

Assuming that:

$$\gamma_T = \lambda + \theta = const \quad \Rightarrow \quad \theta_Z^i = \gamma_T - \lambda_Z^i$$

$r_{P_0}^i$ and $\lambda_{P_0}^i$ is the distance r and the angle λ at the end of the IPP_s $(i-1)$-th stage respectively.

7.1 Simulation

The scenario includes one interceptor against a non-maneuvering target. The interceptor is launched from $(X_{M_0}, Y_{M_0}) = (0, 0)$ with speed of $V_M = 200 \left[\frac{M}{S}\right]$ and path angles which are equal to $\gamma_M(0) = 0[deg]$. The target is launched from $(X_{M_0}, Y_{M_0}) = (2500[m], 0)$ with speed of $V_T = 100 \left[\frac{M}{S}\right]$ and path angles which are equal to $\gamma_T(0) = 90[deg]$. $t_p = 2, \quad t_z = 2$.

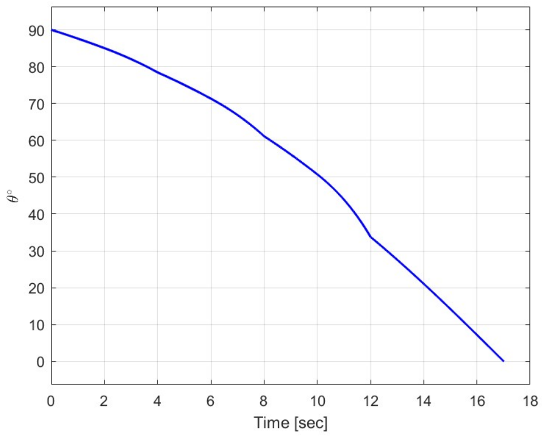

(a) $\theta°$ As a function of time

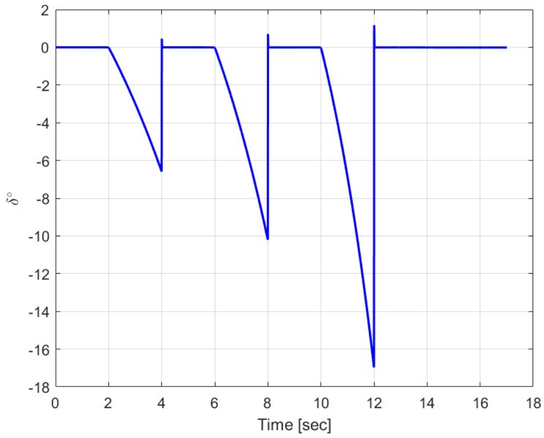

(b) $\delta°$ As a function of time

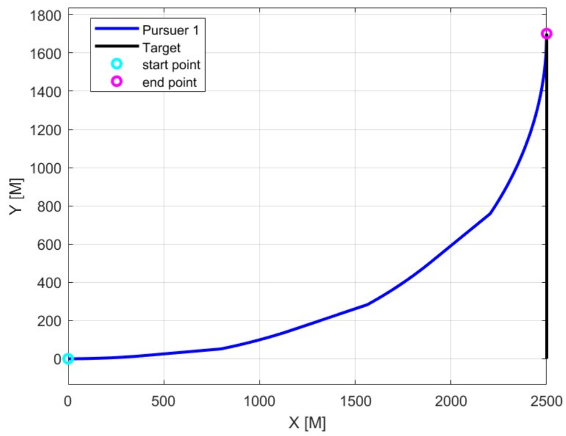

(c) Trajectories

Figure 8: Implementation of IPP for $t_Z = t_P = 2[sec]$.

7.2 Discussion

For the initial conditions of the chosen scenario, if the interceptor had used PP throughout the entire scenario, then θ would have remained positive until the end of the scenario, where it would have been $\theta = 0$. When we perform IPP, during the IPP_s phase, there is a possibility that θ will be negative. This is an undesirable situation, as a $\theta < 0$ indicates that the interceptor is overshooting the target.
Therefore, if during the IPP_s i-th stage of the scenario, $\theta < 0$ is obtained, It is necessary to evaluate the PP_s i-th stage so that the interceptor reaches the target without overshooting.
In the simulation presented in this section, $\theta_Z^4 = -16.2°$ at the end of IPP_s $i = 4$; therefore, it is necessary to extend the PP_s operation $i = 4$ to avoid overshooting.
The extension of the PP_s at $i = 4$ is shown in Fig.8b at $14[sec] < t$, where instead of δ will change, $\delta = 0$, meaning that PP_s be extended.

8 Conclusions

An intermittent pure pursuit guidance concept was presented and investigated. The idea is based on the fact that by applying pure pursuit at regular intervals, it is possible to influence the movement of the pursuer while improving the information on the prey's location by minimizing the disturbances created by the pursuer's movement. The performance of the guidance law was evaluated in nonlinear simulations for a moving target with constant velocity.
It was found that for pursuers with high speed, there is a greater chance of a significant overshoot during the pursuit. This result holds even when t_z increases, in the case where the ratio $\frac{t_p}{t_z}$ and pursuers velocity remains constant. It was also found that the faster the pursuer's speed, the sooner the target will be captured.
Subsequently, a parameter μ was found for which target capture is guaranteed using the IPP method. It was determined that for the ratio $\frac{t_p}{t_z} \geq \mu$, target capture is assured, but it was also shown that even for $\frac{t_p}{t_z} < \mu$, target interception may still occur because the μ parameter is not strict, but guarantees interception for an extreme case.
Afterward, a boundary case was examined where the activation time of IPP_s approaches zero ($t_z \to 0$). It was found that for this case, IPP will approach PP, where the angle delta will be equal to zero throughout the scenario. Finally, a method was presented to prevent overshoot by finding the stage i at which the pursuer would pass the target, while extending the use of PP during the $i-th$ stage of the pursuit scenario.
The advantages of the proposed guidance concept include the simplicity of the geometric principle of PP, relying solely on the angular position of the target. Motion pauses allow computation time to plan the trajectory in the best possible way, while reducing the noise generated by the pursuer's engines in the case of an interceptor or robot.

References

[1] N. A. Shneydor, *Missile Guidance and Pursuit: Kinematics, Dynamics and Control*. Elsevier, Jan. 1998.

[2] I. S. Jeon, J. I. Lee, and M. J. Tahk, "Impact-time-control guidance law for anti-ship missiles," *IEEE Transactions on Control Systems Technology*, vol. 14, pp. 260–266, Mar. 2006.

[3] I. S. Jeon, J. I. Lee, and M. J. Tahk, "Impact-Time-Control Guidance with Generalized Proportional Navigation Based on Nonlinear Formulation," *Journal of Guidance, Control, and Dynamics*, vol. 39, pp. 1885–1890, Aug. 2016.

[4] M. J. Tahk, C. K. Ryoo, and H. Cho, "Recursive time-to-go estimation for homing guidance missiles," *IEEE Transactions on Aerospace and Electronic Systems*, vol. 38, pp. 13–24, Jan. 2002.

[5] H. S. Shin, H. Cho, and A. Tsourdos, "Time-to-go Estimation using Guidance Command History," *IFAC Proceedings Volumes*, vol. 44, pp. 5531–5536, Jan. 2011.

[6] N. Dhananjay and D. Ghose, "Accurate Time-to-Go Estimation for Proportional Navigation Guidance," *Journal of Guidance, Control, and Dynamics*, vol. 37, pp. 1378–1383, July 2014.

[7] S. R. Kumar and D. Ghose, "Sliding mode control based guidance law with impact time constraints," in *2013 American Control Conference*, (Washington, DC), pp. 5760–5765, IEEE, June 2013.

[8] A. Saleem and A. Ratnoo, "Lyapunov-Based Guidance Law for Impact Time Control and Simultaneous Arrival," *Journal of Guidance, Control, and Dynamics*, vol. 39, pp. 164–173, Jan. 2016.

[9] R. Tekin, K. S. Erer, and F. Holzapfel, "Polynomial Shaping of the Look Angle for Impact-Time Control," *Journal of Guidance, Control, and Dynamics*, vol. 40, pp. 2668–2673, Oct. 2017.

[10] R. Tekin, K. S. Erer, and F. Holzapfel, "Adaptive Impact Time Control Via Look-Angle Shaping Under Varying Velocity," *Journal of Guidance, Control, and Dynamics*, vol. 40, pp. 3247–3255, Dec. 2017.

[11] R. Tsalik and T. Shima, "Circular Impact-Time Guidance," *Journal of Guidance, Control, and Dynamics*, vol. 42, pp. 1836–1847, Aug. 2019.

[12] J. I. Lee, I. S. Jeon, and M. J. Tahk, "Guidance law to control impact time and angle," *IEEE Transactions on Aerospace and Electronic Systems*, vol. 43, pp. 301–310, Jan. 2007.

[13] T. H. Kim, C. H. Lee, I. S. Jeon, and M. J. Tahk, "Augmented Polynomial Guidance With Impact Time and Angle Constraints," *IEEE Transactions on Aerospace and Electronic Systems*, vol. 49, pp. 2806–2817, Oct. 2013.

[14] C. H. Brighton and G. K. Taylor, "Hawks steer attacks using a guidance system tuned for close pursuit of erratically manoeuvring targets," *Nature Communications*, vol. 10, p. 2462, June 2019.

[15] C. H. Brighton, A. L. R. Thomas, and G. K. Taylor, "Terminal attack trajectories of peregrine falcons are described by the proportional navigation guidance law of missiles," *Proceedings of the National Academy of Sciences*, vol. 114, pp. 13495–13500, Dec. 2017.

[16] C. H. Brighton, K. E. Chapman, N. C. Fox, and G. K. Taylor, "Attack behaviour in naive gyrfalcons is modelled by the same guidance law as in peregrine falcons, but at a lower guidance gain," *Journal of Experimental Biology*, vol. 224, Mar. 2021.

[17] I. Rañó, "On motion camouflage as proportional navigation," *Biological Cybernetics*, vol. 116, pp. 69–79, Feb. 2022.

[18] K. Ghose, T. K. Horiuchi, P. S. Krishnaprasad, and C. F. Moss, "Echolocating Bats Use a Nearly Time-Optimal Strategy to Intercept Prey," *PLoS Biology*, vol. 4, pp. 865–873, Apr. 2006.

[19] A. F. Haselsteiner, C. Gilbert, and Z. J. Wang, "Tiger beetles pursue prey using a proportional control law with a delay of one half-stride," *Journal of The Royal Society Interface*, vol. 11, June 2014.

[20] M. F. Land and T. S. Collett, "Chasing behaviour of houseflies (Fannia canicularis)," *Journal of comparative physiology*, vol. 89, pp. 331–357, Dec. 1974.

[21] M. J. McHenry, J. L. Johansen, A. P. Soto, B. A. Free, D. A. Paley, and J. C. Liao, "The pursuit strategy of predatory bluefish (*Pomatomus saltatrix*)," *Proceedings of the Royal Society B: Biological Sciences*, vol. 286, Feb. 2019.

[22] A. P. Soto and M. J. McHenry, "Pursuit predation with intermittent locomotion in zebrafish," *Journal of Experimental Biology*, vol. 223, Dec. 2020.